A Method of Phase Control and Impedance Matching of Mutually Coupled ICRF Antennas in LHD

Kenji SAITO, Ryuhei KUMAZAWA, Tetsuo SEKI, Hiroshi KASAHARA, Goro NOMURA,
Fujio SHIMPO, Chihiro TAKAHASHI, Mitsuhiro YOKOTA, and Takashi MUTOH

National Institute for Fusion Science, 322-6 Oroshi-cho, Toki 509-5292, Japan

In the Large Helical Device (LHD), the installation of a pair of ion cyclotron range of frequencies (ICRF) antennas from upper and lower ports is planned. These antennas are geometrically symmetrical and located side by side. By changing the current phase on the straps, the wave number parallel to the magnetic field line can be controlled. However, antenna impedances will also be changed and reflected power will increase due to mutual coupling. For efficient power injection and the protection of tetrode tubes, the parameters of impedance matching devices must be controlled together with the current phase. A method was formulated and trials of phase control and impedance matching were successfully conducted with a simplified two-port dummy antenna.

1. Introduction

In the Large Helical Device (LHD) [1], impedance matching devices with liquid stub tuners [2, 3] are used for high-power and long-pulse ion cyclotron range of frequencies (ICRF) heating. Impedance matching for short-pulse discharge was obtained by measuring reflection coefficients with a directional coupler attached to the outlet of the final power amplifier (FPA) and by adjusting the liquid lengths in the liquid stub tuners during the intervals between shots either manually or automatically [4-6]. The liquid lengths for each shot are calculated using the data from preceding shot with the assumption of constant antenna impedance. For a long-pulse operation, this procedure is carried out continuously. During long-pulse discharges, the reflected power fraction was reduced and kept low enough against variation of antenna impedance [6].

We are planning to install two symmetrical ICRF antennas in the LHD from upper and lower ports. The wave number parallel to the magnetic field line is controllable by adjusting the phase of the current on the straps for the variation of the experiments. Antenna impedance is not constant even if the plasma parameter remains constant when the current ratio including the phase is actively changed due to the mutual coupling between the two antennas. This makes the impedance matching difficult. A decoupler [7, 8] is a useful device; however, tuning is necessary against the variation of plasma parameters.

In Section 2, we discuss the simulation of the electromagnetic field in front of the new ICRF antennas. In Section 3, a method of phase control and impedance

matching of the mutually coupled ICRF antennas is described. Test results of this method are presented in Section 4. The operational region under this method is discussed in Section 5. Section 6 is a summary.

2. Wave number controllability

We simulated the electromagnetic field in front of the new antennas using a High Frequency Structure Simulator (HFSS) [9] and analyzed the S matrix of the antennas. Although real antennas will be twisted along the helical plasma, the simulated antennas were simplified and not twisted. The size of the simulated antennas was as follows:

strap width: 20 cm
antenna width: 44 cm
distance between two antenna centers: 48 cm
strap length: 90 cm
Faraday shield~strap: 1.5 cm
strap~back plate: 6 cm

Power was fed from transmission lines with the characteristic impedance z_c of 50 Ω. An isotropic and homogeneous material with a refraction index of 9 was used as a load instead of plasma, since the HFSS cannot simulate an electromagnetic field in the magnetized plasma. This material approximately simulates a hydrogen plasma with an electron density of 0.4×10^{19} m^{-3} in a magnetic field of 2.75 T at a frequency of 40 MHz, since the refraction index of the fast wave in the plasma is around 9 (from 7 to 10 depending on the wave direction). Power is absorbed on the boundary of the calculation

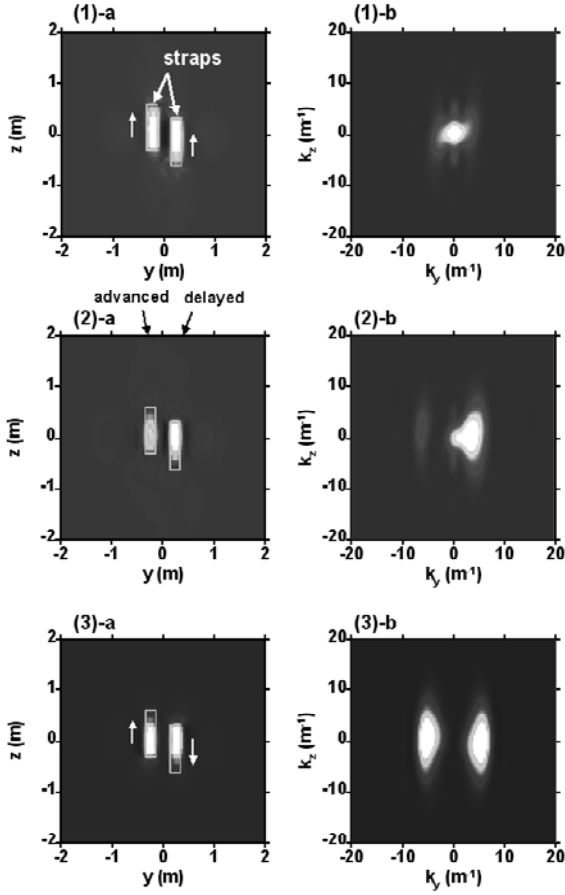*Corresponding author's e-mail: saito@nifs.ac.jp*

Fig. 1 a. Intensities of the component of the Poynting vector directed to the load. Axis y is directed to the magnetic field line and axis z is the direction of the straps. The arrows show the current directions on the straps. b. Fourier spectra of the Poynting vector. Simulation was done for the (1) 0-0, (2) 0-π/2, and (3) 0-π current phases.

space except for the back boundary of the perfect conductor, where the back plate is grounded. Although the antennas are movable to the radial direction, in this simulation, distance between the load and the Faraday shield was fixed at 5 cm. Figures 1-(1)-a, 1-(2)-a, and 1-(3)-a show the intensity of the component of the Poynting vector directed to the load on its surface with a frequency of 40 MHz in the cases of the 0-0, 0-π/2, and 0-π current phases, respectively, with the same forward power from each port. The Poynting vector is intense near the straps. The Fourier spectrum of the Poynting vector changes depending on the phase difference as shown in Figs 1-(1)-b, 1-(2)-b, and 1-(3)-b. The wave number parallel to the magnetic field line is controllable up to approximately 5 m^{-1}. The loading resistance is the impedance at the point at which the voltage is at minimum in the transmission line, and it depends on the current phase on the straps. In the simulation, a symmetrical S matrix was calculated, and the maximum
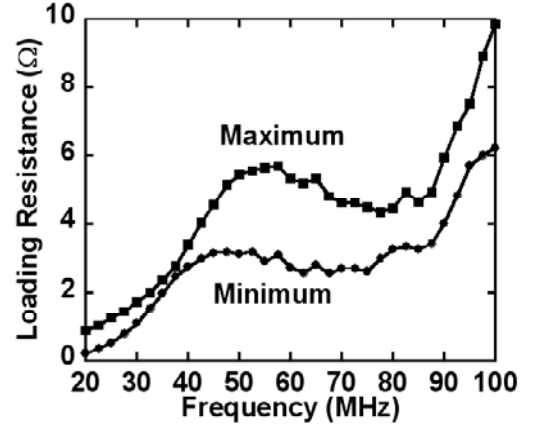

Fig. 2 Maximum and minimum loading resistances as a function of frequency.

and minimum loading resistances of the antennas were determined assuming the same forward power from each port using the following equations:

$$R_{\min} = z_c \frac{1 - (|S_{11}| + |S_{12}|)}{1 + (|S_{11}| + |S_{12}|)}$$

$$R_{\max} = z_c \frac{1 - \|S_{11}| - |S_{12}\|}{1 + \|S_{11}| - |S_{12}\|}$$

(1)

The calculated result is shown in Fig. 2. The difference in the loading resistance is due to the non-diagonal component of the S matrix, i.e., mutual coupling components, and is the cause of the difficulty in impedance matching.

3. A method of phase control and impedance matching

Figure 3 shows a schematic view of the antenna system including matching devices. The two antennas are characterized by a Z matrix, Z_a. Currents at the antenna ports of line 1 and 2 are identified as I_{a1} and I_{a2}, respectively. V_{a1} and V_{a2} are the voltages at the antenna
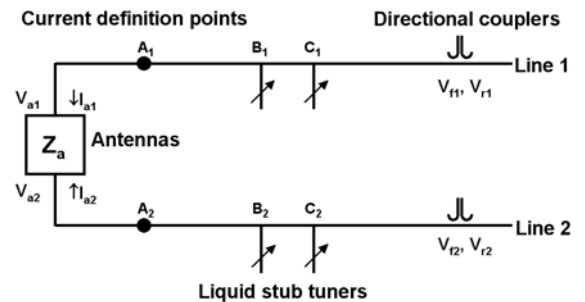

Fig. 3 Schematic view of the antenna system consisting of two lines.

ports. These currents and voltages are related as follows:

$$\begin{pmatrix} V_{a1} \\ V_{a2} \end{pmatrix} = \begin{pmatrix} Z_{a11} & Z_{a12} \\ Z_{a21} & Z_{a22} \end{pmatrix} \begin{pmatrix} I_{a1} \\ I_{a2} \end{pmatrix} \tag{2}$$

Each impedance matching device consists of two or three liquid stub tuners. Directional couplers are inserted at the outlets of the FPAs. The distance between the impedance matching device and the directional coupler is more than 100 m and mechanical measurement is difficult, however it can be measured electrically by changing the liquid length in the closest stub tuner to the directional coupler [4]. In the present impedance matching system, constant impedance between two consecutive shots is assumed. However, by actively changing current phase, this assumption breaks down. The antenna impedances z_{a1} and z_{a2} are derived from Eq. 2 as follows:

$$z_{a1} = Z_{a11} + Z_{a12}\frac{I_{a2}}{I_{a1}}$$
$$z_{a2} = Z_{a21}\frac{I_{a1}}{I_{a2}} + Z_{a22} \tag{3}$$

Therefore antenna impedances change with a complex current ratio I_{a2}/I_{a1} even if the plasma parameter is constant. To predict antenna impedances for the next shot, the Z matrix of antennas must be determined. In general, even if currents (I_{a1}, I_{a2}), and voltages (V_{a1}, V_{a2}), are provided, the components of Z_a cannot be determined from Eq. 2. Therefore, a second measurement of currents and voltages is necessary to determine the Z matrix. However, by assuming geometric symmetry and the reciprocity of the two antennas, Z_a will be symmetrical as $Z_{a11}=Z_{a22}$ and $Z_{a12}=Z_{a21}$. By using these relations, the components are determined as follows:

$$Z_{a11} = Z_{a22} = \frac{I_{a1}V_{a1} - I_{a2}V_{a2}}{I_{a1}^2 - I_{a2}^2}$$
$$Z_{a12} = Z_{a21} = \frac{-I_{a2}V_{a1} + I_{a1}V_{a2}}{I_{a1}^2 - I_{a2}^2} \tag{4}$$

The assumption of geometric symmetry and reciprocity makes it possible to determine Z_a with only one measurement of currents and voltages at the antenna ports, which is preferable for continuous operation. However, in the case of $I_{a1}=\pm I_{a2}$, the Z matrix given in Eq. 4 is not determinable. The impedances $z_{a1}=Z_{a11}\pm Z_{a12}$ and $z_{a2}=\pm Z_{a21}+Z_{a22}$ are determinable, but the ratios, Z_{a12}/Z_{a11} and Z_{a21}/Z_{a22} are unknown. A method of solving this problem is that of using the former ratios at $I_{a1}\neq\pm I_{a2}$.

Figure 4 is a flow chart for obtaining impedance matching with the designated complex current ratio (absolute value and phase). First, the forward wave voltage, $V_{f1,2}$, and reflected wave voltage, $V_{r1,2}$, including
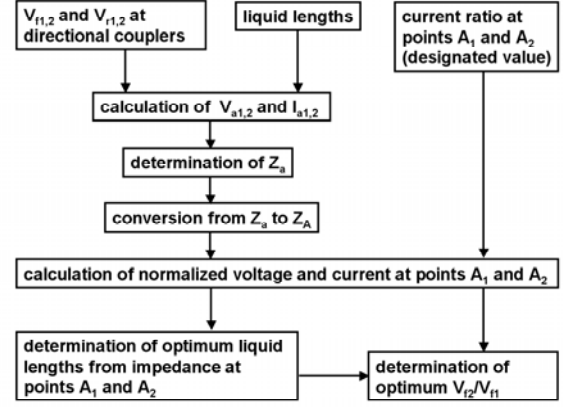

Fig. 4 Flow chart for the determination of the optimum liquid lengths and ratio of forward wave voltages at the directional couplers.

the phase at the directional coupler on each transmission line are measured. In the present impedance matching system, the complex ratio of forward wave voltages, V_{f2}/V_{f1}, is not necessary, but it is used in the new system. The liquid lengths in the stub tuners are also measured. Based on these data and configuration of the antenna system, voltage $V_{a1,2}$ and current $I_{a1,2}$ at the antenna ports are calculated. Then the components of Z_a are determined by the above-mentioned method. Z matrix, Z_A, at the points where the current ratio is defined, is converted from Z_a. The points should be around maximum current on the transmission line to avoid a steep change of phase along lines. The normalized voltages at points A_1 and A_2 are calculated using Z_A and the given complex current ratio. The optimum liquid lengths where the reflected power ratio is at minimum are determined from the impedances V_{A1}/I_{A1} and V_{A2}/I_{A2} with the procedure used in the present impedance matching system [4]. The complex forward wave voltage ratio at directional couplers V_{f2}/V_{f1} is also determined. By adjusting these control parameters for the next shot, impedance matching with the designated complex current ratio will be obtained.

4. Test of phase control and impedance matching with a dummy antenna

The calculation code for the manual control was completed and phase control and impedance matching were conducted with a simplified symmetrical two-port dummy antenna consisting of resisters and connected cables. Two pairs of variable condensers were used instead of liquid stub tuners. The experimental conditions were the following:

frequency: 30 MHz
electric lengths between antenna ports and points $B_{1,2}$:
5.027 m

electric lengths between points, $A_{1,2}$ and $B_{1,2}$: 0.188 m (voltages were measured at quarter wavelength shifted points to antenna from points, $A_{1,2}$.)
electric lengths between points, $B_{1,2}$ and $C_{1,2}$: 0.777 m
electric lengths between points, $C_{1,2}$ and directional couplers: 2.584 m
characteristic impedance of transmission lines: 50 Ω

4-1. Test of phase shift

We first tested whether the current phase shifts properly without increase of reflection. In the initial condition, reflections are zero. The ratio of forward waves is $|V_{f2}/V_{f1}|=1.16$ with a phase of 83.8°. The current ratio at points A_1 and A_2, $|I_{A2}/I_{A1}|$ was 1.06 with a phase of 91.6°. The equivalent stub tuner length normalized by wavelength A is defined by $z = jz_c \tan(2\pi A)$, where z is the impedance at the junctions and z_c is the characteristic impedance of 50 Ω. The measurement with a network analyzer gave A_{ant}=0.405 (antenna side), A_{osc}=0.285 (oscillator side) for line 1 and A_{ant}=0.379, A_{osc}=0.367 for line 2. The calculated Z matrix of the dummy antenna was determined as follows:

$$Z_a = \begin{pmatrix} 15.2+12.9j & 5.06+0.27j \\ 5.06+0.27j & 15.2+12.9j \end{pmatrix} \quad (5)$$

The calculated current ratio at the points A_1 and A_2 was 1.12 with a phase of 90.3°, which agreed well with measured current ratio. Based on this condition, only the phase of V_{f2}/V_{f1} was decreased by 128.8° from 83.8° to -45.0°. The reflection ratios at the directional couplers are increased significantly from 0 to 0.35 for line 1 and to 0.29 for line 2. The measured current ratio at points A_1 and A_2 was 1.22 and the phase decreased by 163.3°, which is much larger than the phase shift of V_{f2}/V_{f1}. Therefore, adjustment based on calculation is necessary. In the case of a designated current ratio of 1 with a phase of -45°, the calculated setting values for the impedance matching using the above-mentioned Z matrix of the dummy antenna are as follows:

$|V_{f2}/V_{f1}| = 0.979$, phase(V_{f2}/V_{f1}) = -38.6°
line 1: A_{ant} = 0.351, A_{osc} = 0.354
line 2: A_{ant} = 0.383, A_{osc} = 0.310

By adjusting these parameters to the calculated one, low reflection ratios of 0.025 for line 1 and 0.009 for line 2 were obtained. The measured current ratio was then 1.01 and the phase was -44.1°. This result means that impedance matching with the designated current ratio and phase was achieved.

4-2. Test of convergence

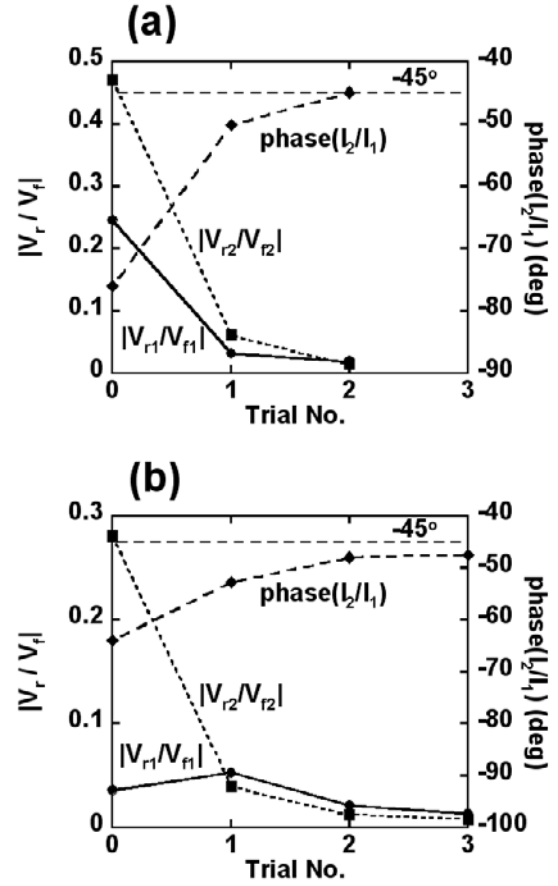We next repeated the procedure shown in Fig. 4 to

Fig. 5 Convergences of reflection ratio and current phase for the (a) symmetrical and (b) asymmetrical cases.

test whether the reflection ratio converges to zero even if impedance matching is not obtained in one trial. Figure 5-(a) shows the reduction of the reflection ratio using a symmetrical dummy antenna. The initial reflection ratio was set large, but by repeating the procedure with the designated current ratio of 1 and the phase of -45°, the reflection ratio was reduced to almost zero and the current phase difference converged to the designated phase difference in the second trial. After this convergence, a cable 27.2 cm in electric length was inserted in port 2 of the dummy antenna to deliberately make the dummy antenna asymmetrical. In the first trial, the reflection ratio of port 1 increased slightly, but that of port 2 decreased drastically, and both then decreased almost to zero (Fig. 5-(b)). This property of convergence allows small errors in measurement or asymmetry of ICRF antennas for impedance matching. The phase of I_2/I_1 converged to -47.5° in the asymmetrical case. The small difference from the designated value of -45° is thought to be due to asymmetry caused by the insertion of the cable.

5. Operational region in the current ratio

Figures 6-(a) and (b) are contour maps of the loading

resistances for lines 1 and 2, respectively, which were calculated using the Z matrix of Eq. 5. Loading resistances change with current ratio and phase. In the gray region in the figure, the loading resistance is negative, i.e., the output power is negative. This method is based on power control from two transmitters. Since the negative output power cannot be controlled, the region is the non-operational region. To operate in this region, a decoupler is useful, since loading resistance will be positive and constant. The adjustment of the decoupler can also be carried out with the calculation using the deduced Z matrix of the antenna.
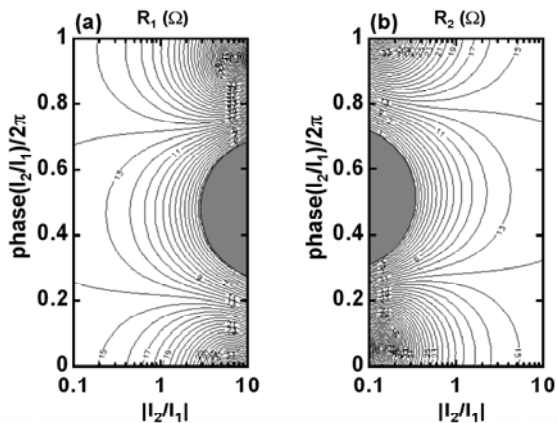

Fig. 6 Contour map of loading resistances in (a) line 1 and (b) line 2 as a function of current ratio and phase. The loading resistance is negative in the gray region.

6. Summary

Phase control and impedance matching of the mutually coupled dummy antenna were successfully demonstrated based on the calculation of the symmetrical Z matrix of the antenna. This method can be utilized in the present real-time feedback system by adding measurement of the phase difference between the forward waves and inserting a controllable phase shifter and attenuators in low-power feed lines.

References

[1] O. Motojima et al., Nucl. Fusion **47**, S668 (2007).
[2] R. Kumazawa et al., Rev. Sci. Instrum. **70**, 2665 (1999).
[3] K. Saito et al., Rev. Sci. Instrum. **72**, 2015 (2001).
[4] K. Saito et al., J. Korean Phys. Soc. **49,** S187 (2006).
[5] K. Saito et al., Fusion Eng. Des. **81**, 2837 (2006).
[6] K. Saito et al., Fusion Eng. Des. **83**, 245 (2008).
[7] R. Majeski et al., Fusion Eng. Des. **24**, 159 (1994).
[8] C.K. Hwang et al., Fusion Eng. Des. **45**, 127 (1999).
[9] Ansoft Announce HFSS v11,
     IEEE MTT-S INTERNATIONAL MICROWAVE SYMPOSIUM, HONOLULU, HI - June 5, 2007
     http://www.ansoft.com/news/press_release/070605.cfm